Received: 28 July 2021 | Revised: 24 August 2021 | Accepted: 3 October 2021

DOI: 10.1002/mp.15278

RESEARCH ARTICLE

MEDICAL PHYSICS

A new emittance selection system to maximize beam transmission for low-energy beams in cyclotron-based proton therapy facilities with gantry

Vivek Maradia[1,2] | **David Meer**[1] | **Damien Charles Weber**[1,3,4] | **Antony John Lomax**[1,2] | **Jacobus Maarten Schippers**[5] | **Serena Psoroulas**[1]

[1] Center for Proton Therapy, Paul Scherrer Institute, Villigen, Switzerland

[2] Department of Physics, ETH Zurich, Zurich, Switzerland

[3] Department of Radiation Oncology, University Hospital Zurich, Zurich, Switzerland

[4] Department of Radiation Oncology, University Hospital Bern, University of Bern, Bern, Switzerland

[5] Large accelerator facility, Paul Scherrer Institute, Villigen, Switzerland

Correspondence
Vivek Maradia, Center for Proton Therapy, Paul Scherrer Institute, Villigen, Switzerland.
Email: Vivek.maradia@psi.ch

Funding information
PSI's CROSS funding scheme

[Correction added on 8 Jun, 2022, after first online publication: Projekt DEAL funding statement has been added.]

Abstract

Purpose: In proton therapy, the potential of using high-dose rates in the cancer treatment is being explored. High-dose rates could improve efficiency and throughput in standard clinical practice, allow efficient utilization of motion mitigation techniques for moving targets, and potentially enhance normal tissue sparing due to the so-called FLASH effect. However, high-dose rates are difficult to reach when lower energy beams are applied in cyclotron-based proton therapy facilities, because they result in large beam sizes and divergences downstream of the degrader, incurring large losses from the cyclotron to the patient position (isocenter). In current facilities, the emittance after the degrader is reduced using circular collimators; however, this does not provide an optimal matching to the acceptance of the following beamline, causing a low transmission for these energies. We, therefore, propose to use a collimation system, asymmetric in both beam size and divergence, resulting in symmetric emittance in both beam transverse planes as required for a gantry system. This new emittance selection, together with a new optics design for the following beamline and gantry, allows a better matching to the beamline acceptance and an improvement of the transmission.

Methods: We implemented a custom method to design the collimator sizes and shape required to select high emittance, to be transported by the following beamline using new beam optics (designed with TRANSPORT) to maximize acceptance matching. For predicting the transmission in the new configuration (new collimators + optics), we used Monte Carlo simulations implemented in BDSIM, implementing a model of PSI Gantry 2 which we benchmarked against measurements taken in the current clinical scenario (circular collimators + clinical optics).

Results: From the BDSIM simulations, we found that the new collimator system and matching beam optics results in an overall transmission from the cyclotron to the isocenter for a 70 MeV beam of 0.72%. This is an improvement of almost a factor of 6 over the current clinical performance (0.13% transmission). The new optics satisfies clinical beam requirements at the isocenter.

Conclusions: We developed a new emittance collimation system for PSI's PROSCAN beamline which, by carefully selecting beam size and divergence asymmetrically, increases the beam transmission for low-energy beams in current state-of-the-art cyclotron-based proton therapy gantries. With these

improvements, we could predict almost 1% transmission for low-energy beams at PSI's Gantry 2. Such a system could easily be implemented in facilities interested in increasing dose rates for efficient motion mitigation and FLASH experiments alike.

KEYWORDS
beam optics, efficient treatment delivery, FLASH, high-dose rates, proton therapy gantry

1 | INTRODUCTION

Over the past two decades, proton therapy experienced remarkable developments and has become a credible option in radiotherapy to treat certain types of cancers. The most advanced, and nowadays the most used method to deliver the dose is spot scanning or pencil beam scanning (PBS)[1,2] first introduced on a gantry in a clinical setting at PSI in the 1990s. PBS typically provides improved dose conformity and healthy tissue sparing when compared to equivalent photon plans.[3–5] However, PBS is especially prone to uncertainties caused by anatomical changes and motion during the treatment, which may compromise its effectiveness.[6–8] Hence, the use of this technology is limited in the case of moving tumors. Such treatments will necessarily require some means for mitigating the interplay effect between the motions in the patient and the beam delivery,[9] the most common motion mitigation techniques being breath-hold,[10,11] rescanning,[12–15] and gating.[16]

Treatment delivery time with PBS depends both on the beam-on time and the dead time (the time required to change energy layers and/or lateral position) between pencil beams. As such, PBS irradiation with high-intensity beams will reduce beam-on time and thus shorten total delivery times, making motion mitigation techniques such as breath-hold or gating more efficient and patient-friendly. Additionally, higher beam intensities will permit efficient delivery of hypo-fractionated treatments and will be an important enabler of proton FLASH techniques.[17–19]

Most of the proton therapy facilities use a cyclotron, which extracts proton beams at fixed energy. However, to spread the dose over the depth of the tumor, different beam energies are needed for the treatment (70–230 MeV). In a cyclotron-based facility, the energy is lowered by passing the beam through energy-degrading material(s) (so-called energy degraders). However, due to scattering in the degrader, for low-energy beams, the emittance after the degrader is in the range of few hundreds of π*mm*mrad.[20,21] Additionally, due to range straggling in the degrader, the momentum spread of the beam will also increase. Therefore, to minimize beam losses in the beamline, it is necessary to use beam emittance selection collimators after the degrader and momentum selection slits in the energy selection system (ESS) to restrict the emittance and momentum spread to the requirement of the following beamline or gantry.[20,22] Currently, all cyclotron-based proton therapy facilities transport a maximum emittance of 30 π*mm*mrad through the beamline[22–27] (in this work, beam sizes, divergences, and emittances are expressed as 2σ values), which limits the transmission of low-energy beams. For example, for the lower energies transported by the Gantry 2 at our institute (70–100 MeV), transmission from the cyclotron to the isocenter is of the order of only 0.1%, limiting beam intensity and therefore increasing treatment times, particularly for superficial tumors.

One way to achieve higher intensity beams at the isocenter is to transport a higher emittance through the following beamline and gantry. For example, in a beam optics study, we have recently shown the potential of allowing higher emittance to be transported through the gantry using a larger beam size and smaller divergence at the gantry entrance.[28,29] In this study, we propose to extend this transmission increase to the beam transport line between degrader and gantry. Such a solution should minimize transmission losses through the whole beam transport, while still achieving clinically acceptable beams at the isocenter.

For proton beam delivery with a gantry, it is required to have the same beam properties at the isocenter for all gantry angles. The most straightforward method to achieve this is to have the same emittance (same beam size and divergence) in both planes at the entrance of the gantry.[24] In general, in most cyclotron-based gantry facilities, two round-shaped collimators, positioned after the degrader, are used (designated as C1 and C2 in Figure 1) which then provide the same beam size and divergence in both planes, which is then symmetrically imaged to the gantry entrance point.[22,24–26,30,31] Due to the alternating focusing signs of quadrupole lenses and bending magnets, the requirements for beam size and beam divergence at the start of the beam transport after the degrader can be quite different for obtaining a maximum transmission and symmetric emittance. A round-shaped collimator limits the emittance in both planes in the same way, to achieve the symmetric emittance requirement, but at the same time, it limits the emittance in one plane more than necessary.

In this paper, we propose an emittance selection based on asymmetric beam size and divergence selection and demonstrate its impact on transmissions

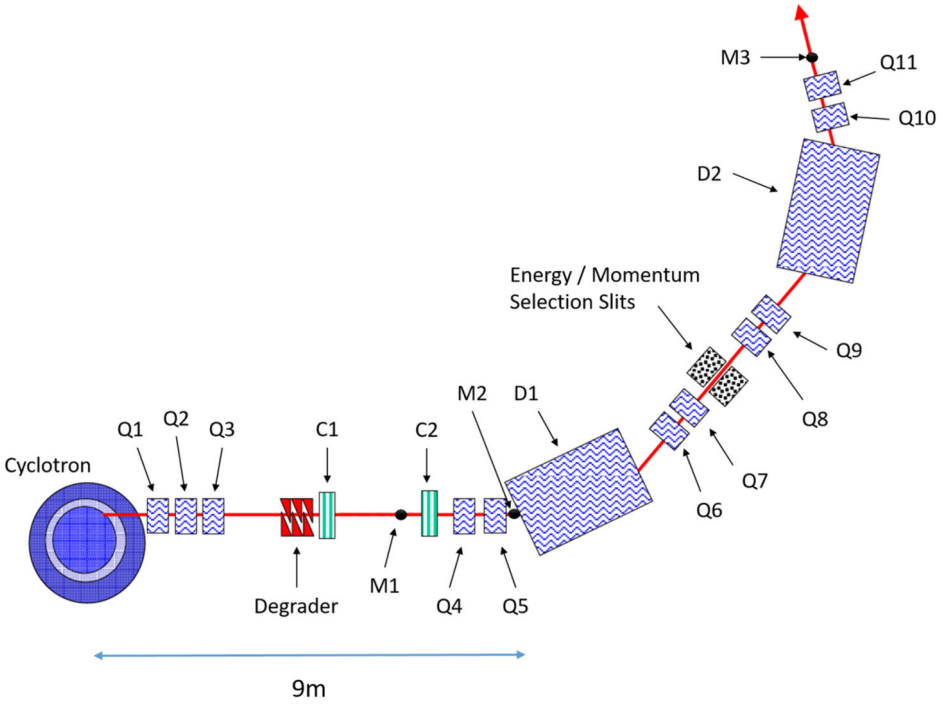

FIGURE 1 Schematic representation of the PROSCAN beam line's energy selection system. (Q = Quadrupole magnet, D = Dipole/Bending magnet, C1 = Beam size selection collimator, C2 = Beam divergence selection collimator and, M= Beam current and beam profile monitor)

through simulations on the PSI proton therapy facility PROSCAN.[32] Using asymmetric collimation, a higher (but still symmetric) beam emittance can be transported through the beamline. To calculate the transmission improvements of this design, we have performed Monte Carlo simulations using BDSIM[33] and have validated the model using measurements performed at the PSI's Gantry 2 facility. After reaching a satisfactory description from the BDSIM model, we have used it to predict the performance of the new collimator scheme in our beamline. As we mainly want to improve transmission for low-energy beams, we focus here only on the lowest energy transported through our gantry (70 MeV). However, as all proton therapy facilities worldwide have similar limitations of maximum beam size in one transverse plane and maximum divergence in another transverse plane, we expect the method described in this paper to be applicable to other cyclotron-driven facilities as well.

2 | MATERIALS AND METHODS

2.1 | Reference beam optics

The reference beam optics (currently used at PSI) of the PROSCAN beamline were designed to have point-to-point imaging from the degrader exit at beam size selection collimator C1 (as shown in Figure 1) to the coupling point of Gantry 2 with intermediate images. Collimator C1 defines a 3 mm beam size, while collimator C2 defines a 10 mrad divergence in both planes. The beam optics has then been designed such that all magnet settings scale similarly with the beam momentum set by the ESS. The gantry beam optics was also designed to provide a point-to-point focus in both planes with a 1:1 imaging from the coupling point of the gantry to the isocenter. The system is designed such that it provides complete achromaticity of the transported beam in both the beam transport line and in the gantry.

With the reference beam optics, we lose almost 98.5% beam in the degrader and the collimator system (i.e., until M2) due to the only 30 π*mm*mrad emittance resulting from the round collimators C1 and C2. In addition, due to the momentum selection slits necessary to match the momentum spread of the beam to the beamline acceptance ($\Delta p/p = \pm 1\%$), we end up losing almost 99.77% beam by the time the beam reaches M3 at the end of the ESS. The beam transport from the end of the ESS to the coupling point however is very efficient (almost zero losses). Finally, there is local transmission of about 58% through the gantry. As such, the overall transmission from the cyclotron to the isocenter is in the order of 0.1%.

2.2 | Required aperture sizes of the asymmetric collimators

The main requirement of the emittance selection collimators is to select the same emittance in both transverse planes. We illustrate how this is performed on our beamline (the ESS is schematically shown in Figure 1).

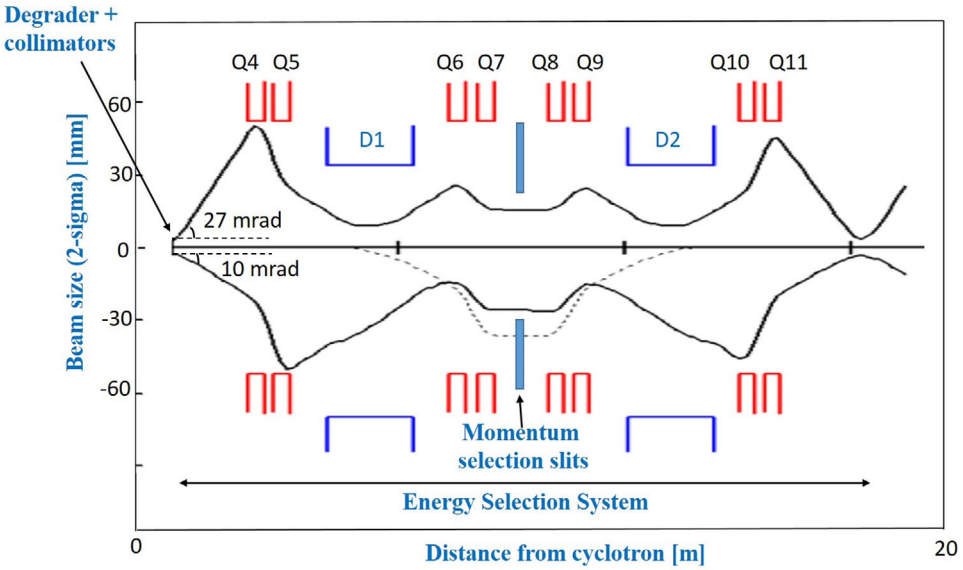

FIGURE 2 Beam optics transporting 30 π*mm*mrad (3 mm beam size and 10 mrad divergence) in X-plane and 81 π*mm*mrad (3 mm, 27 mrad) in Y-plane through ESS. Beam envelope shows the beam size in 2-sigma values and the dispersion (dashed line) (The lower half shows beam envelope in X-plane (bending plane) and the upper half shows envelope in Y-plane

TABLE 1 Required aperture radius of collimator C1 and C2 to achieve 100 π*mm*mrad emittance in both planes

Collimator C1 radius (mm)		Collimator C2 radius (mm)	
X-plane	Y-plane	X-plane	Y-plane
13.5	3.5	12.4	33.5

TABLE 2 Required beam sizes from collimator C1 and divergences from collimator C2 to achieve 100 π*mm*mrad emittance in both planes

	Beam Size from Collimator C1 (mm)	Divergence from Collimator C2 (mrad)	Emittance (π*mm*mrad)
X-plane	10	10	100
Y-plane	3.7	27	100

After the degrader, quadrupole Q4, the first quadrupole after the degrader, is used to focus the beam in the vertical (*Y*) plane. As quadrupole Q4 focuses the beam in the *Y*-plane, it will defocus the beam in the horizontal (*X*) plane. However, although defocused in the *X*-plane, the beam size in the *X*-plane is limited by the aperture of the following quadrupole Q5, leading to different maximum divergence acceptances in both planes. With the 3 mm beam size defined by collimator C1, the maximum possible divergences are 27 mrad in the *Y*-plane and 10 mrad in the *X*-plane (Figure 2). In the *Y*-plane however, the beamline allows a divergence almost three times higher compared to the *X*-plane.

As the Gantry 2 can transport 100 π*mm*mrad emittance,[28] we have designed the collimator system C1–C2 to select 100 π*mm*mrad in both planes too. We, therefore, selected the beam divergence selection collimator (C2) aperture such, to have the maximum acceptable divergences in both planes, being 10 mrad and 27 mrad in the *X* and *Y*-plane, respectively. To also obtain equal emittance in both planes, the beam size in the *Y*-plane must be three times smaller than the beam size in the *X*-plane. For this, we design collimator C1 such that it selects a 10 mm beam size in the *X*-plane, and a 3.7 mm beam size in the *Y*-plane (Tables 1 and 2). The used collimator apertures are given in Table 1. As we first cut the beam using collimator C1, the shape of the beam after the collimator is not Gaussian. Therefore, to optimize the aperture of collimator C1 an iterative process of testing different collimator apertures and determining their equivalent Gaussian parameters was performed until the required beam size after the collimator was reached.

2.3 | New beam optics design with asymmetric collimators

The beam optics has been designed by using the matrix formalism code TRANSPORT.[34] To design new beam optics for the PROSCAN beamline to transport the higher emittance (100 π*mm*mrad) resulting from the use of asymmetric collimators, we used similar point-to-point imaging as used in the reference beam optics. However, to maximize the transmission through the beamline and gantry, we have adapted the imaging factors for the new beam optics. As this starts with different beam sizes in the two transverse planes at collimator C1, different imaging in both planes is needed to achieve the same beam size (16 mm) at the coupling point. For the fixed part of the beamline (before the gantry), we

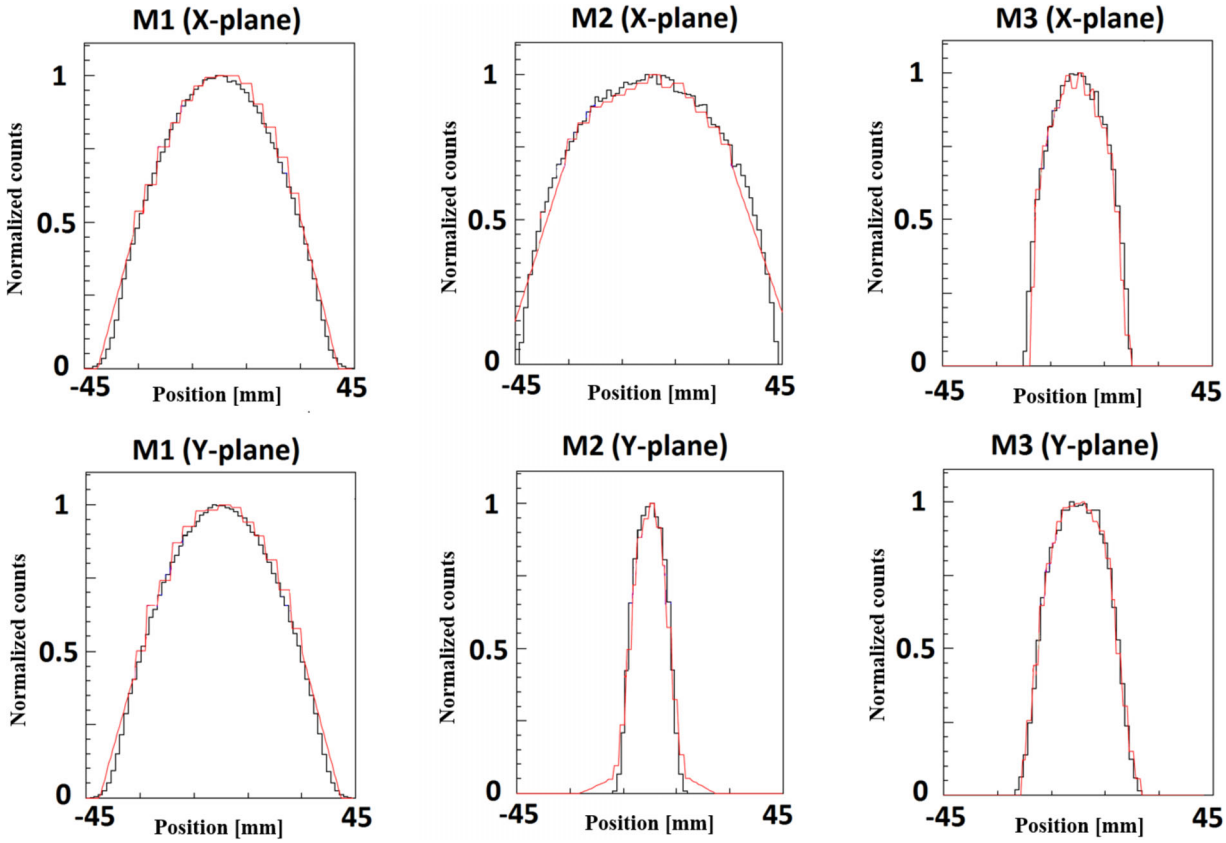

FIGURE 3 Results of beam profile measurements. The measured profiles are shown in red (light line), the BDSIM simulation results in black (dark line)

have used 1:2 imaging in the *X*-plane and 1:5 imaging in the *Y*-plane between collimator C1 and the coupling point. The Gantry 2 beam optics is then set at 2:1 imaging between the gantry coupling point and the isocenter to get 8 mm beam size at the isocenter image point (in vacuum). The momentum spread of the beam is similar to the reference beam optics.

2.4 | Monte Carlo simulations

TRANSPORT cannot predict beam losses along the beamline. To calculate the transmission of the new beam optics, Monte Carlo simulations, based on beamline settings optimized with TRANSPORT, are required. In this work, these have been performed using the BDSIM 1.4.1[33] Monte Carlo simulation toolkit. BDSIM is based on the Geant4 toolkit [16] and is capable of simulating a wide variety of beamline components and magnets with Geant4 geometry, and can predict beam losses in particle accelerator/beamline components with high accuracy.[35] We have therefore built a model of PSI's PROSCAN beamline and Gantry 2 in BDSIM. The calculations have been performed with the physics list based on recommended modules for proton therapy (*G4EmStandardPhysics_option4, G4HadronPhysicsQGSP_BIC_HP, G4StoppingPhysics, G4HadronElasticPhysicsHP, G4EmStandardPhysics-WVI*).[36–40] BDSIM has then been used to calculate the beam losses along the beamline, which can then be compared with relevant experimental data. To minimize statistical error, simulations with 10 million initial particles have been performed. To experience the systematic uncertainty due to the choice of the physics model in transmission calculation, we repeated the simulations using two different physics models, G4HadronPhysicsQGSP_BIC_AllHP and G4HadronPhysicsQBBC. Transmission differences between the two physics models were within ±3%. Post-processing of the simulation data has been performed using ROOT v6.22[41] and MATLAB v9.6[42] scripts.

3 | RESULTS

3.1 | Validation of BDSIM model against measurement

In the PROSCAN beamline, there are many strip chamber monitors along the beamline which measure the profiles and the current (= intensity) of the beam.[43] The BDSIM simulations of the reference beam optics, simulated signals in all profile monitors which could then be compared to experimental data. The profiles of three

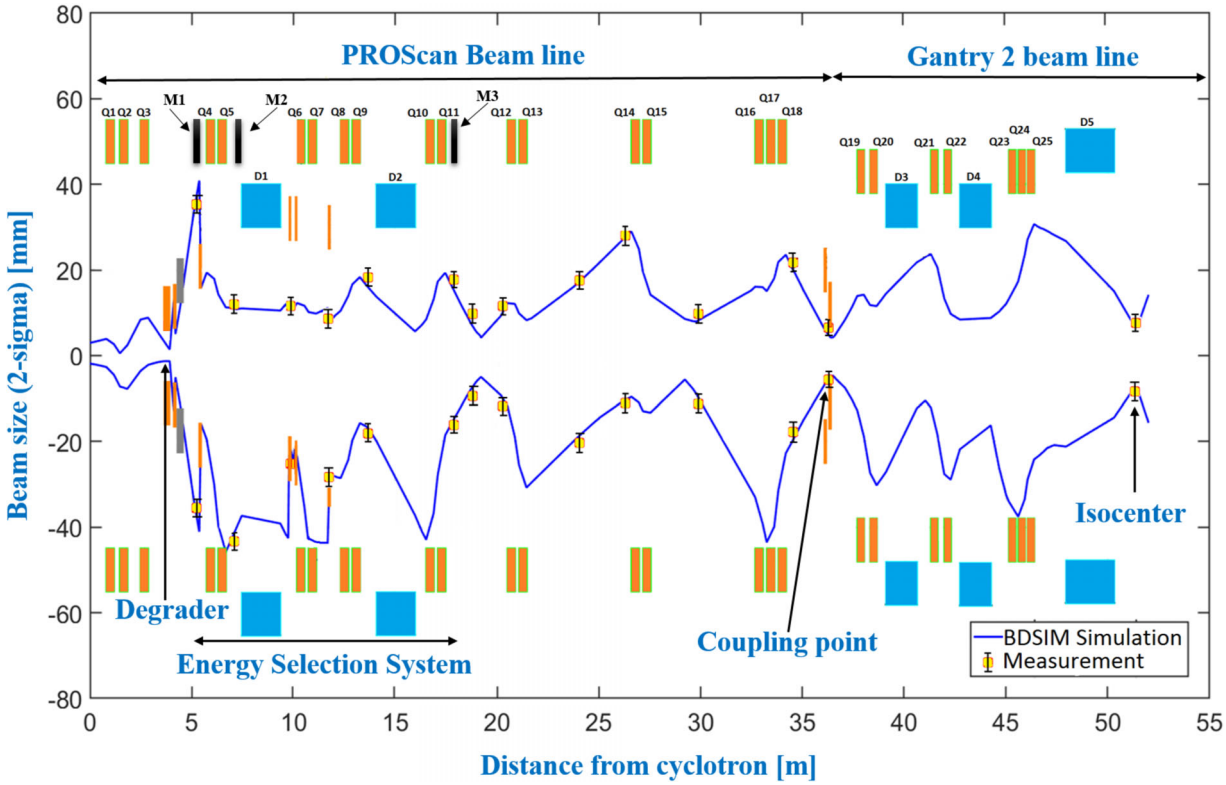

FIGURE 4 Beam envelope from BDSIM simulation for PSI's reference beam optics for 70 MeV beam. The lower half shows the beam envelope in X-plane (bending plane) and the upper half shows the envelope in Y-plane. Yellow squares show measured beam size with black error bars (gaussian fitting error)

TABLE 3 Comparison between measured and simulated transmission along the beamline for reference beam optics. The transmission is expressed as a percentage of the beam intensity extracted from the cyclotron

	M1	M2	M3	Coupling point	isocenter
BDSIM Simulation	10 ± 0.3%	1.47 ± 0.04%	0.23 ± 0.007%	0.22 ± 0.007%	0.13 ± 0.004%
Measurements	10.1 ± 0.7%	1.46 ± 0.1%	0.21 ± 0.015%	0.21 ± 0.015%	0.13 ± 0.002%

important monitors (elements M1–3 shown in Figure 1), located behind the collimators (C1 and C2) and the ESS, where most of the beam is lost, are shown in Figure 3. For each monitor, the particle distribution predicted by the BDSIM is directly compared with the measured profile. Measured and simulated profiles were found to be in good agreement.

Besides the qualitative comparison in Figure 3, an analysis was performed of the beam transport from cyclotron exit to the isocenter of the Gantry 2, as shown in Figure 4. This compares the beam size calculated with BDSIM with measurements performed at the profile monitors along the PROSCAN beamline. For these, the measured beam size has been extracted using a Gaussian fit, indicating that simulated and measured beam sizes also match along the beamline. Note that even when the beam profiles are non-Gaussian, the beam shape is always similar in both simulations and measurements.

Transmission measurements through the ESS have been performed at three different beamline positions using current monitors M1, M2, and M3. In addition, transmission has also been measured at the coupling point (gantry entrance) and isocenter.

As shown in Table 3, transmission calculation of reference beam optics using BDSIM simulation matches the measured transmission. The overall transmission from the cyclotron to the isocenter is in the order of 0.1%. The agreement between the measurement results and the simulated profiles and transmission, as listed in Figures 3 and 4, and Table 3, indicates that the accuracy of the simulated transmissions is much better than 10%, sufficient for the purpose of this work.

3.2 | Transmission improvements with asymmetric collimators

Figure 5 compares the reference beam optics (30 π*mm*mrad emittance) using round collimators and with the beam optics using elliptically shaped asymmetric collimators (100 π*mm*mrad). Although this new beam

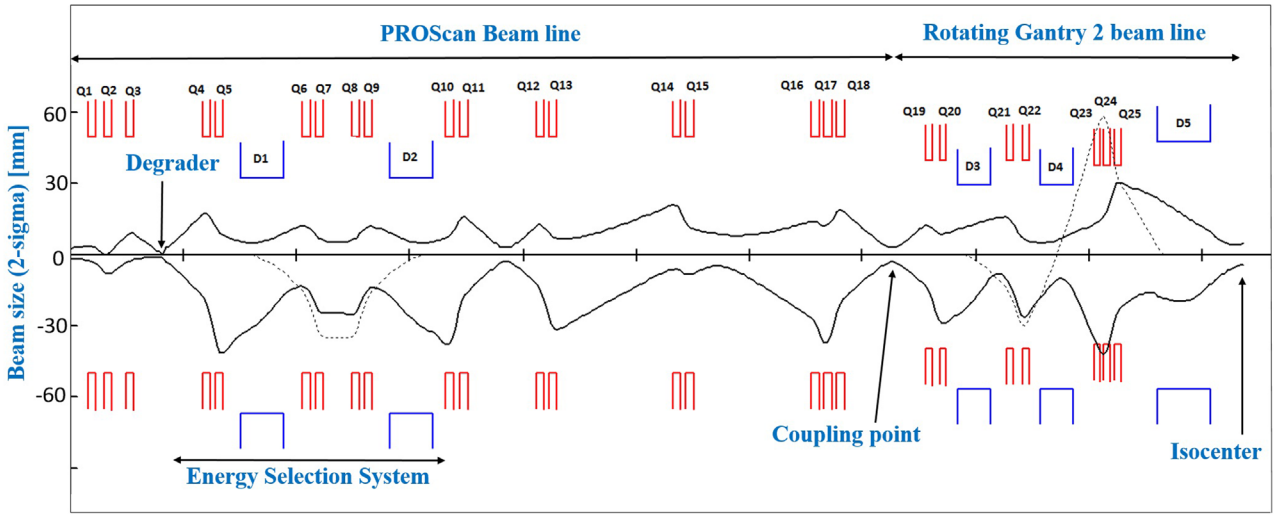

(a) Reference beam optics transporting 30 pi*mm*mrad emittance using round collimators

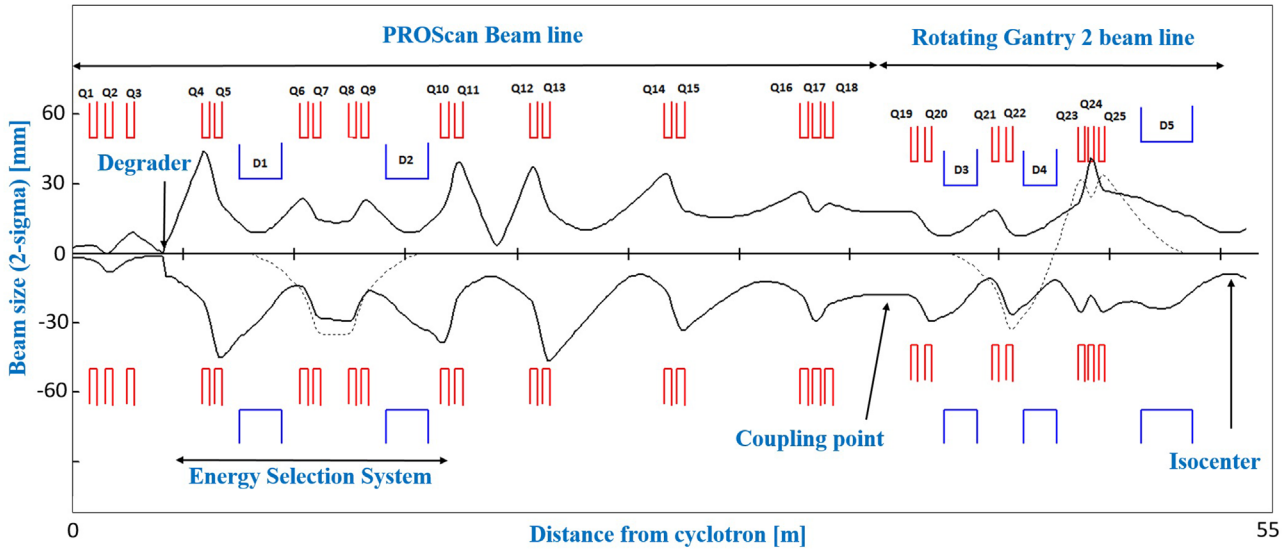

(b) New beam optics transporting 100 pi*mm*mrad emittance using an asymmetric collimators

FIGURE 5 Part (a) shows reference beam optics with two round-shaped symmetric phase space selection collimators. Part (b) shows newly developed beam optics with two asymmetric phase space selection collimators. Beam envelope shows the beam size in 2-sigma values and the dispersion (dashed line) along the PROSCAN beamline and Gantry 2 (The lower half shows beam envelope in X-plane (bending plane) and the upper half shows envelope in Y-plane.)

TABLE 4 Simulation results of the transmission using round collimators (30 π*mm*mrad emittance transport) and using asymmetric collimators (100 π*mm*mrad emittance transport). Transmission values are from the cyclotron to different locations along the beamline

	M1	M2	M3	Coupling point	isocenter
Reference beam optics	10 ± 0.3%	1.47 ± 0.04%	0.23 ± 0.007%	0.22 ± 0.007%	0.13 ± 0.004%
New beam optics	15 ± 0.45%	5.5 ± 0.165%	1.22 ± 0.037%	1.2 ± 0.036%	0.72 ± 0.022%

optics was designed with TRANSPORT (envelopes shown in Figure 5(b)), BDSIM has been used to estimate the transmission along the beamline.

At monitor M2, losses of almost 94.5% in beam intensity after the asymmetric emittance selection collimators have been estimated, versus a loss of 98.5% with the reference optics (Table 4). As asymmetric collimation enables a larger emittance with an improved matching to the acceptance of the following beamline, this results in a higher transmission. As such, with an emittance of 100 π*mm*mrad in both planes, we are able to achieve 1.22% transmission through the ESS instead of

0.23% in the reference beam optics. Similar to the reference beam optics, there are no losses between the end of the ESS and the coupling point and for both cases, transmission through the gantry is about 60%. With an asymmetric collimation system, we thus predict an overall transmission from the cyclotron to the isocenter for 70 MeV beam of 0.72%, compared to 0.13% in the reference beam optics, corresponding to an increase of almost a factor of 6 in beam current reaching the patient. However, this comes at a cost on beam size with the simulated beam size in the air for the reference optics at isocenter being 11.2 $\pm$ 0.6 mm, whereas for the asymmetric beam optics, beam size at isocenter is 17.2 $\pm$ 0.7 mm, representing an increase of about 50%. With the new system, we could achieve a maximum of 6 nA beam current at the isocenter for 70 MeV beam compared to 1 nA with the reference beam optics.

4 | DISCUSSION

We have demonstrated that an asymmetric collimator system for emittance selection, aiming at selecting asymmetric beam sizes and beam divergences following the degrader in a cyclotron-based proton therapy facility, can achieve substantially higher transmissions for low-energy beams. This approach overcomes the limitations of typically used circular collimators, by separately matching horizontal and vertical emittances to the acceptance of the downstream beamline. Using this design based on asymmetric collimators, we have shown that up to 100 π*mm*mrad emittance could be transported in both planes through the beamline. In a BDSIM simulation of the PSI PROSCAN beamline, we have found that this approach increases the low-energy transmission by almost a factor of 6 compared to reference beam optics. In the simulation, we assumed that the new collimator system is located at the same position as the current collimator system; such a change could thus be implemented easily in clinical practice. By comparing PSI's system with other cyclotron-driven proton therapy facilities, we expect that a similar asymmetric collimator system will be applicable in other cyclotron-based facilities to increase the transmission for low-energy beams. However, the magnitude of the transmission increase will be facility dependent due to differences in distances, apertures, materials, and cyclotron energies.

Using asymmetric collimators to minimize losses will mostly improve the transmission at the lower energies used in proton therapy. There might however be some effects also at the higher energies. For these (e.g., in the range 180–230 MeV), the beam size and divergence after the degrader will be lower than the beam sizes selected in the *X*-plane and the divergence selected in the *Y*-plane using collimators C1 and C2, respectively. Because of this, for high-energy beams, we will not completely fill the aperture of the collimators, resulting in different emittances in the *X* and *Y* planes. One way to overcome this deviation is to increase the beam size (e.g., by magnetic defocusing) and divergence (either by magnetic defocusing or by using a scattering foil made of high-*Z* material) of the incoming beam before or in the energy degrader. This will increase the beam size and divergence of the high-energy beam, but will then cover the collimators C1 and C2 compactly. In this way, we will get the same emittance in both planes even for high-energy beams, although this could result in a less-optimal transmission of high-energy beams through the collimator system. However, since higher energies naturally have lower losses, the two effects will counteract each other, thus reducing the otherwise large energy-dependent variation of the beam intensity reaching the patient.

Because of the higher emittance transported using asymmetric collimators, the beam size at the isocenter will be 1.5 times larger compared to the reference beam optics, which will have an inevitable effect on the lateral penumbra. However, this might only be a limitation for static tumors as larger beam sizes might be useful in the context of motion mitigation.[44] Larger beam sizes could also be of advantage by enabling a reduction of the number of spots required to cover the target volume, potentially shortening the total delivery time even further, and might also provide even more robustness to the treatment plan. The beam sizes obtained with the new optics, anyway, are still acceptable from a clinical point of view, since they are compatible with those used in other facilities.[45,46] However, the beam size at the isocenter is dependent on gantry beam optics and it will be investigated as a continuation of this work.

In addition to the asymmetric collimator, the choice of degrader material also has an impact on the divergence after the degrader and thus on transmission. For example, degraders made of boron carbide[20] or beryllium[22] could bring an additional 20%–30% increase in transmission with respect to a graphite degrader (one of the most commonly used material). At PSI, we are investigating the possibility of using a boron carbide degrader, which, if combined with the asymmetric collimation system presented here, could result in about a factor of 7 higher transmission with respect to the reference optics.

5 | CONCLUSION

In summary, we have demonstrated that the transport of higher emittance beams through the beamline can substantially increase low-energy beam transmission by improved matching of the beam emittance between elliptically shaped emittance selection collimators and improved beam optics with a larger resulting beam size at the coupling point. The resulting improved dose rates could improve the treatment of moving tumors,

by extending proton therapy applications to a more efficient implementation of breath-hold, gating, and rescanning. Shorter delivery times will also allow an efficient implementation of hypo-fractionation regimes and eventually contribute to reducing the proton therapy treatment cost.[47,48] It may also help to reach FLASH dose rates. This approach therefore could open a wide range of possibilities for both current and future proton therapy practice.

ACKNOWLEDGMENTS

We thank Dr. Rudolf Doelling for his support in the measurements. We acknowledge the help of the PSI cyclotron operation group, PSI vacuum group, and PSI radiation protection group. This work is funded by PSI's CROSS funding scheme. Open Access Funding provided by Lib4RI Library for the Research Institutes within the ETH Domain Eawag Empa PSI and WSL.

CONFLICT OF INTEREST

The authors declare that there is no conflict of interest that could be perceived as prejudicing the impartiality of the research reported.

DATA AVAILABLILITY STATEMENT

The data will be available to interested researches upon request and under a confidentiality agreement, as they contain sensitive information about a PSI product.

REFERENCES

1. Pedroni E, Bacher R, Blattmann H, et al. The 200-Mev proton therapy project at the Paul Scherrer Institute: conceptual design and practical realization. *Med Phys*. 1995;22(1):37-53. https://doi.org/10.1118/1.597522.
2. Lin S, Boehringer T, Coray A, Grossmann M, Pedroni E. More than 10 years experience of beam monitoring with the Gantry 1 spot scanning proton therapy facility at PSI. *Med Phys*. 2009;36(11):5331-5340. https://doi.org/10.1118/1.3244034.
3. Lomax AJ, Bortfeld T, Goitein G, et al. A treatment planning inter-comparison of proton and intensity modulated photon radiotherapy. *Radiother Oncol*. 1999;51(3):257-271. https://doi.org/10.1016/S0167-8140(99)00036-5.
4. Ladra MM, Edgington SK, Mahajan A, et al. A dosimetric comparison of proton and intensity modulated radiation therapy in pediatric rhabdomyosarcoma patients enrolled on a prospective phase II proton study. *Radiother Oncol*. 2014;113(1):77-83. https://doi.org/10.1016/j.radonc.2014.08.033.
5. Eaton BR, MacDonald SM, Yock TI, Tarbell NJ. Secondary malignancy risk following proton radiation therapy. *Front Oncol*. 2015;5(Nov):1-6. https://doi.org/10.3389/fonc.2015.00261.
6. Bert C, Grözinger SO, Rietzel E. Quantification of interplay effects of scanned particle beams and moving targets. *Phys Med Biol*. 2008;53(9):2253-2265. https://doi.org/10.1088/0031-9155/53/9/003.
7. Seco J, Robertson D, Trofimov A, Paganetti H. Breathing interplay effects during proton beam scanning: simulation and statistical analysis. *Phys Med Biol*. 2009;54(14). https://doi.org/10.1088/0031-9155/54/14/N01.
8. Phillips MH, Pedroni E, Blattmann H, Boehringer T, Coray A, Scheib S. Effects of respiratory motion on dose uniformity with a charged particle scanning method. *Phys Med Biol*. 1992;37(1):223-234. https://doi.org/10.1088/0031-9155/37/1/016.
9. Chang JY, Zhang X, Knopf A, et al. Consensus guidelines for implementing pencil-beam scanning proton therapy for thoracic malignancies on behalf of the PTCOG Thoracic and Lymphoma Subcommittee. *Int J Radiat Oncol Biol Phys*. 2017;99(1):41-50. https://doi.org/10.1016/j.ijrobp.2017.05.014.
10. Hanley J, Debois MM, Mah D, et al. Deep inspiration breath-hold technique for lung tumors: the potential value of target immobilization and reduced lung density in dose escalation. *Int J Radiat Oncol Biol Phys*. 1999;45(3):603-611. https://doi.org/10.1016/S0360-3016(99)00154-6.
11. Dueck J, Knopf AC, Lomax A, et al. Robustness of the voluntary breath-hold approach for the treatment of peripheral lung tumors using hypofractionated pencil beam scanning proton therapy. *Int J Radiat Oncol Biol Phys*. 2016;95(1):534-541. https://doi.org/10.1016/j.ijrobp.2015.11.015.
12. Mori S, Inaniwa T, Furukawa T, Zenklusen S, Shirai T, Noda K. Effects of a difference in respiratory cycle between treatment planning and irradiation for phase-controlled rescanning and carbon pencil beam scanning. *Br J Radiol*. 2013;86(1028). https://doi.org/10.1259/bjr.20130163.
13. Schätti A, Zakova M, Meer D, Lomax AJ. Experimental verification of motion mitigation of discrete proton spot scanning by re-scanning. *Phys Med Biol*. 2013;58(23):8555-8572. https://doi.org/10.1088/0031-9155/58/23/8555.
14. Zenklusen SM, Pedroni E, Meer D. A study on repainting strategies for treating moderately moving targets with proton pencil beam scanning at the new gantry 2 at PSI. *Phys Med Biol*. 2010;55(17):5103-5121. https://doi.org/10.1088/0031-9155/55/17/014.
15. Klimpki G, Zhang Y, Fattori G, et al. The impact of pencil beam scanning techniques on the effectiveness and efficiency of re-scanning moving targets. *Phys Med Biol*. 2018;63(14). https://doi.org/10.1088/1361-6560/aacd27.
16. Ohara K, Okumura T, Akisada M, et al. Irradiation synchronized with respiration gate. *Int J Radiat Oncol Biol Phys*. 1989;17(4):853-857. https://doi.org/10.1016/0360-3016(89)90078-3.
17. Nesteruk KP, Psoroulas S. Flash irradiation with proton beams: beam characteristics and their implications for beam diagnostics. *Appl Sci*. 2021;11(5):1-11. https://doi.org/10.3390/app11052170.
18. Jolly S, Owen H, Schippers M, Welsch C. Technical challenges for FLASH proton therapy. *Phys Med*. 2020;78(September):71-82. https://doi.org/10.1016/j.ejmp.2020.08.005.
19. van de Water S, Safai S, Schippers JM, Weber DC, Lomax AJ. Towards FLASH proton therapy: the impact of treatment planning and machine characteristics on achievable dose rates. *Acta Oncol (Madr)*. 2019;58(10):1463-1469. https://doi.org/10.1080/0284186X.2019.1627416.
20. Gerbershagen A, Baumgarten C, Kiselev D, Van Der Meer R, Risters Y, Schippers M. Measurements and simulations of boron carbide as degrader material for proton therapy. *Phys Med Biol*. 2016;61(14):N337-N348. https://doi.org/10.1088/0031-9155/61/14/N337.
21. Anferov V. Energy degrader optimization for medical beam lines. *Nucl Instrum Methods Phys Res A*. 2003;496:222-227. https://doi.org/10.1016/S0168-9002(02)01625-X.
22. Van Goethem MJ, Van Der Meer R, Reist HW, Schippers JM. Geant4 simulations of proton beam transport through a carbon or beryllium degrader and following a beam line. *Phys Med Biol*. 2009;54(19):5831-5846. https://doi.org/10.1088/0031-9155/54/19/011.
23. Flanz J. B. Large medical gantries. Proceedings Particle Accelerator Conference, 1995, Vol.3, pp. 2004-2008. https://doi.org/10.1109/PAC.1995.505434.
24. Yves J, Gantry comprising beam analyser for use in particle therapy. US Patent 9,289,624 B2. 2010. https://patentswarm.com/patents/US9289624B2.

25. Schippers JM. Beam-transport systems for particle therapy. *Cern Yellow Reports Sch Proc*. 2017;1(May):241-252. 10.23730/CYRSP-2017-001.241.
26. Chen W, Yang J, Qin B, et al. Transmission calculation and intensity suppression for a proton therapy system. *Nucl Instrum Methods Phys Res A*. 2018;881:82-87. https://doi.org/10.1016/j.nima.2017.10.047.
27. Zeng XH, Zheng JX, Song YT, et al. Beam optics study for energy selection system of SC200 superconducting proton cyclotron. *Nucl Sci Tech*. 2018;29(9):1-8. https://doi.org/10.1007/s41365-018-0462-5.
28. Maradia V, Meer D, Giovannelli AC, et al. New gantry beam optics solution for minimizing treatment time in cyclotron-based proton therapy facilities. PTCOG 2021 Conference. Particle Therapy Co-Operative Group; 2021. https://doi.org/10.3929/ethz-b-000497120.
29. Maradia V, Meer D, Giovannelli HAC, et al. A novel beam optics concept to maximize the transmission through cyclotron-based proton therapy gantries. *Proc IPAC2021*. JACoW Publishing; 2477-2479. http://doi.org/10.18429/JACoW-IPAC2021-TUPAB407.
30. Juargen D & Helmut P (2016). U.S. Patent Number US2016314929A. Washington, DC: U.S. Patent and Trademark Office.
31. Liang Z, Chen W, Qin B, Liu X, Liu K, Zha J. Design of the energy selection system for proton therapy based on GEANT4*. *CYC 2016-Proc 21st Int Conf Cyclotrons their Appl*. 2016;2016:30-32.
32. Schippers JM, Dölling R, Duppich J, et al. The SC cyclotron and beam lines of PSI's new protontherapy facility PROSCAN. *Nucl Instrum Methods Phys Res B*. 2007;261(suppl 1-2):773-776. https://doi.org/10.1016/j.nimb.2007.04.052.
33. Agapov I, Blair GA, Malton S, Deacon L. BDSIM: a particle tracking code for accelerator beam-line simulations including particle–matter interactions. *Nucl Instrum Methods Phys Res A* 2009;606(3):708-712. https://doi.org/10.1016/j.nima.2009.04.040.
34. Brown KL, Carey DC, Iselin FC, Rothacker F. *Transport, a Computer Program for Designing Charged Particle Beam Transport Systems*. CERN; 1980. https://doi.org/10.5170/CERN-1980-004.
35. Nevay LJ, Boogert ST, Garcia-Morales H, et al. Beam delivery simulation: BDSIM automatic Geant4 models of accelerators. IPAC 2016: Proceedings of the 7th International Particle Accelerator Conference. 2016. Inspire;3098-3100.
36. Psoroulas S, Meer D, Oponowicz E, Owen H. Mean excitation energy determination for Monte Carlo simulations of boron carbide as degrader material for proton therapy. *Phys Med*. 2020;80(April):111-118. https://doi.org/10.1016/j.ejmp.2020.09.017.
37. Jarlskog CZ, Paganetti H. Physics settings for using the Geant4 toolkit in proton therapy. *IEEE Trans Nucl Sci*. 2008;55(3):1018-1025. https://doi.org/10.1109/TNS.2008.922816.
38. Grevillot L, Frisson T, Zahra N, et al. Optimization of GEANT4 settings for proton pencil beam scanning simulations using GATE. *Nucl Instrum Methods Phys Res B*. 2010;268(20):3295-3305. https://doi.org/10.1016/j.nimb.2010.07.011.
39. Fuchs H, Vatnitsky S, Stock M, Georg D, Grevillot L. Evaluation of GATE/Geant4 multiple Coulomb scattering algorithms for a 160 MeV proton beam. *Nucl Instrum Methods Phys Res B*. 2017;410:122-126. https://doi.org/10.1016/j.nimb.2017.08.006.
40. Resch AF, Elia A, Fuchs H, et al. Evaluation of electromagnetic and nuclear scattering models in GATE/Geant4 for proton therapy. *Med Phys*. 2019;46(5):2444-2456. https://doi.org/10.1002/mp.13472.
41. Brun R, Rademakers F. ROOT: An object oriented data analysis framework. *Nucl Instrum Methods Phys Res A* 2020;389:81-86.
42. MATLAB version 9.6.0.1072779 (R2019a). 2019.
43. Dölling R. Profile, current, and halo monitors of the PROSCAN beam lines. *AIP Conf Proc*. 2004;732:244-252. https://doi.org/10.1063/1.1831154.
44. Grassberger C, Dowdell S, Sharp G, Paganetti H. Motion mitigation for lung cancer patients treated with active scanning proton therapy. *Med Phys*. 2015;42(5):2462-2469. https://doi.org/10.1118/1.4916662.
45. Almhagen E, Boersma DJ, Nyström H, Ahnesjö A. A beam model for focused proton pencil beams. *Phys Med* 2018;52(June):27-32. https://doi.org/10.1016/j.ejmp.2018.06.007.
46. Shamurailatpam D, Manikandan A, Ganapathy K, et al. Characterization and performance evaluation of the first-proton therapy facility in India. *J Med Phys*. 2020;45(2):59-65. https://doi.org/10.4103/jmp.JMP_12_20.
47. Verma V, Mishra MV, Mehta MP. A systematic review of the cost and cost-effectiveness studies of proton radiotherapy. *Cancer*. 2016;122. https://doi.org/10.1002/cncr.29882.
48. Lievens Y, Pijls-Johannesma M. Health economic controversy and cost-effectiveness of proton therapy. *Semin Radiat Oncol*. 2013;23(2):134-141. https://doi.org/10.1016/j.semradonc.2012.11.005.

SUPPORTING INFORMATION

Additional supporting information may be found in the online version of the article at the publisher's website.

How to cite this article: Maradia V, Meer D, Weber DC, Lomax AJ, Schippers JM, Psoroulas S. A new emittance selection system to maximize beam transmission for low-energy beams in cyclotron-based proton therapy facilities with gantry. *Med Phys*. 2021;48:7613–7622. https://doi.org/10.1002/mp.15278